'93 한국자동제어학술회의논문집 (1993.10.20~22)

초음파 센서를 이용한 로봇의 실내 평면 구조 인식

고중협, 김완주, 정명진°
한국과학기술원 전기 및 전자공학과

A Method of Floor Plan Recognition by Using Ultrasonic Sensors for Mobile Robot Navigation

Joong Hyup Ko, Wan Joo Kim, and Myung Jin Chung°
Dept. of Electrical Engineering, KAIST

Abstract

When a mobile robot moves around autonomously without man-made landmarks, it is essential to recognize the placement of surrounding objects especially for current position estimation, obstacle avoidance, or homing into the work station. In this paper, we propose a novel approach to recognize the floor plan for indoor mobile robot navigation using ultrasonic time-of-flight method. We model the floor plan as a collection of polygonal plane objects and recognize the floor plan by locating edges and vertices of the objects. The direction is estimated by the patterns of transmission beam and reception sensitivity of the ultrasonic transducer, and the distance is estimated by the correlation detection method. We show the validity of the proposed approach through experimental results and discuss the resolution and the accuracy of the estimation of direction and distance.

1. Introduction

For a mobile robot's autonomous navigation and task accomplishment, it is important to recognize the configuration of the surroundings. Especially for indoor navigation on the two-dimensional environment, the floor plan recognition is essential for current position estimation, obstacle avoidance, or homing to the work station.

Of the many kinds of sensors that a mobile robot uses to recognize the environment, vision sensor, laser range finder, ultrasonic sensor, and infrared sensor are most prevalent today. Among them, the ultrasonic sensor is known to have numerous advantages such as measuring distance directly without any affection to the environment, simple signal processing in relatively short period of time, low power consumption, small physical size, and no hazard to human.

Because of these advantages, there have been reported many methods to use the ultrasonic sensor for mobile robot's environment recognition. We classify the previous approaches into the following four categories. The first category includes the early approaches that assume narrow beamwidth and scattered reflection on rough surfaces [1,2]. The environment is recognized by assuming a point at the distance estimated from the first echo on the line-of-sight. Since most surfaces in real environment are specular and the beamwidth is not that narrow at typical acoustic carrier frequency, the applicability of this approach is rather limited.

The approches in the second category assume a curved or linear object along the arc defined by the beamwidth and the distance to the nearest object[3,4]. Because the post-processing cannot eliminate artifacts completely, and the objects beyond the nearest object cannot be recognized, environment recognition with these approaches can be misleading and insufficient.

The third category includes many grid based approaches that confirm the largest free space in front of the ultrasonic sensor defined by the beamwidth and the distance to the nearest object[5,6]. As the free space recognized at each measurement is always fan-shaped, the approaches are not appropriate to recognize the detail of the environment.

Included in the final category are various approaches based on the physical priciples of acoustic wave propagation[7,8]. Because only the first echo is used in [7], it is required that no more than one object may exist in the scan direction, and no two objects may be closely located. Due to these constraints, the recognition range is severely limited. In [8], the matching of echoes received by the three receivers is performed following the maximum likelihood principle, therefore objects need to be separated sufficiently for succesful matching in proportion to the distances between the receivers. But as the receivers come closer, the recognition accuracy and discriminating capability are also reduced.

In this paper, we propose a novel recognition approach by using ultrasonic sensors based on the pulsed-echo method. The proposed approach does not limit the recognition range to the nearest object nor includes uncertainty in the matching of the correlated echoes. We first define our model of the environment in Section 2, then explain how to estimate the directions and the distances to the reflectors in Section 3 and 4. In Section 4, we also explain our differentiating alrogithm between

reflector types. Some experimental results are presented in Section 5 to show the validity of the proposed approach. We discuss the limitations of our method in Section 6, and Section 7 concludes our paper.

2. Model of the Environment

We model the indoor environment by polygonal prisms and assume that the prisms extend from the floor to the height above the ultrasonic sensor system. Therefore the environment to be recognized is the floor plan modeled as a collection of horizontal polygons. Following the convention, we call the convex and concave vertices of a polygon an *edge* and a *corner* respectively, and the edge of a polygon a *wall*. But our definitions of corner and edge are broader than those of [13] in which edge and corner correspond only to *right-angled* vertices. Fig. 1 shows these geometrical elements of our environment model with a ultrasonic transducer.

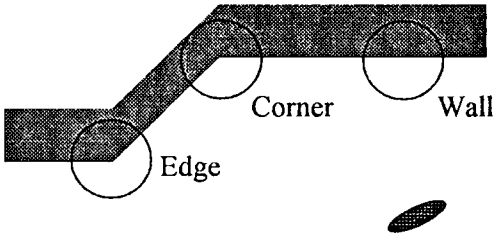

Fig. 1 Wall, edge, and corner.

Since the roughness of the many indoor surfaces in the real world is less than the typical wavelength of the ultrasonic wave, the surfaces behave as specular objects, and we may assume that edges of the polygons in floor plan are all specular. For a specular polygon, there can be two modes of acoustic wave propagation from a transmitter to a receiver; diffraction at edges and corners, and reflection at walls.

1) Diffraction at edge and corner:
As the dimensions of vertices of a polygon is smaller than the wavelength of the ultrasonic wave, diffraction occurs at the vertices to all directions. To a receiver, the received echo from a vertex is identical to the ultrasonic wave transmitted from a point source located at the vertices. Fig. 2 shows the diffraction at an edge, where the shaded area represents the echo rays received by a receiver.

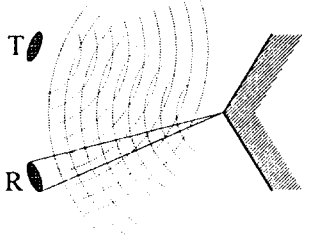

Fig. 2 Diffraction at an edge.

2) Reflection at Edge:
If the size of a wall is longer than the wavelength of a ultrasonic wave as in the usual cases, the incident wave reflects at the wall. As the incident and the reflecting angles are identical, and the acoustic rays are linear, there exist finite volume of rays that are received by a receiver. Fig. 3 shows the echo reflecting from a wall. The shaded area represents the echo rays received by a receiver.

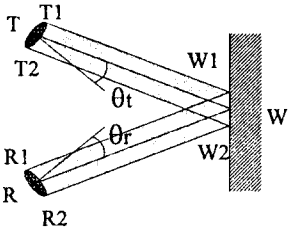

Fig. 3 Reflection at a wall.

3. Direction Estimation

3.1 Physical Model of the Transducer

In this paper, we use the Polaroid ultrasonic transducer which acts both as a transmitter and a receiver[9]. From acoustics, it is known that the transducer can be modeled as a circular plane piston in an infinite baffle[12]. When the transducer vibrates with simple harmonic motion, the radiated acoustic pressure at a point in the far field shown in Fig. 4 is a function of range r and of angular deviation from the transducer orientation θ [10]. The pressure pattern is described as

$$p(r,\theta) = (P_0/r) \cdot \left[\frac{2J_1(ka\sin\theta)}{ka\sin\theta}\right],$$

where P_0 is a constant gain, $J_1(\cdot)$ is the Bessel function of the first kind of order 1, k is the wave number, and a is the radius of the transducer. Here we can see that all of the angular dependence of p is in the bracketed term which is even symmetric with the normal axis (θ=0) along which the maximum pressure occurs.

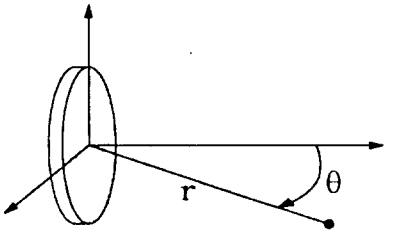

Fig. 4 A far-field point from the transducer.

In the far field, the first off-axis local minimum of the Bessel function defines the *beamwidth* θ_0 as

$$\theta_0 = \sin^{-1}\frac{0.61\lambda}{a},$$

where λ is the wavelength of the acoustic wave[11].

If a time limited signal is applied to the transducer, we can approximate the pressure at a far-field point as a Gaussian function of[11]

$$p(r,\theta) = (P_0/r)\cdot e^{-2\theta^2/\theta_0^2}.$$

The first term at right shows that the pressure is inversely proportional to the range. If we use a time-variable gain amplifier to compensate this attenuation, the pressure is a function only of the deviation angle. After normalization, it becomes

$$p(\theta) = e^{-2\theta^2/\theta_0^2}. \quad (*)$$

According to the acoustic reciprocity principle, the reception sensitivity has the same pattern with that of the transmitted wave pressure[10]. Therefore, we can express the receiver sensitivity as

$$s(\theta) = e^{-2\theta^2/\theta_0^2}.$$

Here, θ is the angle between the normal axis of the receiver and the propagation direction of incident wave.

3.2 Echo Amplitude Pattern

With a transmitter-receiver pair, we determine the direction to a wall or a vertex of a polygon. Firstly, we consider the echo propagated through reflection at an edge. Theoretically, the rays representing the acoustic wave radiated from a transmitter are not parallel. But as the cross section of a receiver located in the far field is much smaller than the beamwidth of a transmitter, we can approximate the acoustic wave arriving at the receiver as a set of parallel rays. We call the area occupied by these receiving rays a *propagation channel.* We show the propagation channel from a transmitter T to a receiver R in Fig. 2, where the propagation channel is defined by the parallel bounding paths of $T_1 - W_1 - R_1$ and $T_2 - W_2 - R_2$.

The amplitude of an echo received through propagation channel depends on the amplitude of transmitted wave radiated into the channel and the sensitivity of the receiver with respect to the channel. By assuming use of the time-variable gain amplifier and unity reflectance coefficient, we get the echo amplitude of

$$a(\theta) = e^{-2\theta_t^2/\theta_0^2}\cdot e^{-2\theta_s^2/\theta_0^2},$$

where θ_t and θ_s are the inclination angles of transmitter and receiver with respect to the propagation channel. The maximum amplitude is acquired when $\theta_t = 0$ or when $\theta_s = 0$. In other words, when the transmitter or the receiver looks directly to the point W in Fig. 2, the echo has the maximum magnitude. We name the point W a *reflection point.*

Now, we consider the echo propagated through diffraction at a vertex. Similar to the reflected echo, the diffracted wave at a vertex has the greatest amplitude when the transmitter's normal direction aims at the vertex, and the maximum amplitude of an echo is acquired when the receiver looks directly to the vertex. A vertex is also a reflection point.

3.3 Amplitude Peak Estimation

We estimate the direction to a reflection point by rotating transmitter(receiver) and measuring the echo amplitude at each angle of rotation. From storage and processing time considerations, we need to take this sampling step size as much as possible not to miss an echo[12].

We first consider the case where only transmitter is rotated. Because the echo amplitude pattern is even symmetric, the direction of $\theta_t = 0$ can be found by fitting a even curve to the sampled echo amplitudes. As the echo has the maximum amplitude at $\theta_t = 0$ direction, we call this direction an *peak amplitude direction.* For simplicity, we use a quadratic polynomial as the even symmetric fitting function. If the measured echo amplitude is contaminated by a noise of zero mean, the fitting curve still provides the optimal estimation of the amplitude peak direction. Fig. 5 shows a sampled amplitude of an echo from a convex vertex and the fitted quadratic polynomial curve.

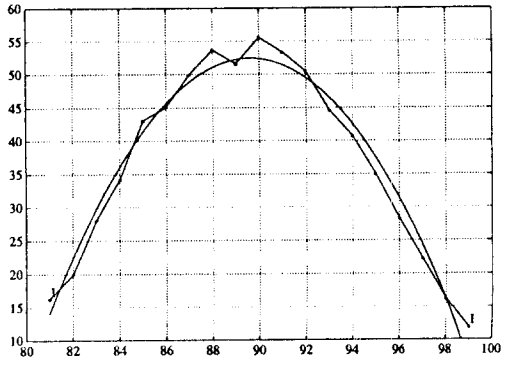

Fig. 5 Echo amplitude samples and quadratic polynomial fitting curve.

If we rotate only the receiver with a fixed transmitter, the peak amplitude direction can be found similarly. When a transducer acts both as a transmitter and a receiver, we can model the transducer as a pair of real and imaginary transducers which rotate by the same angle[13]. Therefore, the echo amplitude pattern is still even symmetric, and the peak amplitude direction can be found by the same method.

3.4 Differentiation between Edge and Corner

It is known that an edge can be easily differentiated from a wall or a corner based on the echo amplitude[12]. But wall and right angled corner are known to be indistinguishable by single transducer, as they have identical image of the transducer[11]. Unlike the method of [11], the transmitter in our method rotates at a fixed position, therefore there exists a difference between the echo propagation paths for wall and right angled corner. For example, if we use a transmitter to find an unidentified reflection point X as shown in Fig. 6, we can identify the type by employing another transducer as a receiver.

The signal propagation path for wall is T-W-R. For corner, the signal path will be T-C1-C2-R. Therefore, the echo amplitude is maximum when the transmitter's normal axis aims at W in case of a wall and C1 in case of a right angle corner.

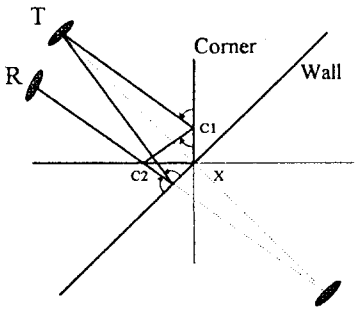

Fig. 6 Wall and right angled corner.

4. Distance Estimation

To determine the distance to a reflecting object, we measure the time between pulse transmission and echo reception. Fig. 7 shows the pulse signal we use. The pulse is modulated by 50 KHz sinusoidal wave, and has even symmetric envelope and duration about 0.5 milliseconds.

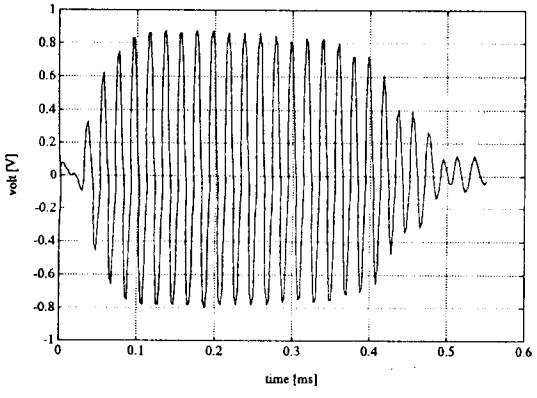

Fig. 7 Pulse signal.

Conventionally, only the first echo pulse has been utilized in the pulsed-echo method. Because the first echo pulse corresponds to the nearest object from the sensor, objects beyond the nearest can not be recognized. Moreover, as the reflection point on an object is not always at the center of the arc formed by the first echo from that object, we can not assume that an object exists in the direction of the arc center[13].

Therefore, we need to process the entire echo signal to take into account the subsequent echo pulses as well as the first one. For this, we use the matched filter.

As the electrical pulse signal applied to an ultrasonic transducer does not maintain the signal shape, we can not use the electrical signal as the impulse response of the matched filter. Instead, we use the pulse signal received by a receiver facing a transmitter directly. It is known that the transmitter-receiver pair facing each other directly has impulsive impulse response[13]. If we negelect the shape deformation through the air, we may assume that an echo signal is a addition of the pulse signal we use.

The output of a matched filter is a correlation between input signal and impulse response of the filter.

For our pulse signal, the correlation output of the matched filter is a monotonously increasing and decreasing signal with a unique peak. In Fig. 8, we show the autocorrelation output of the matched filter.

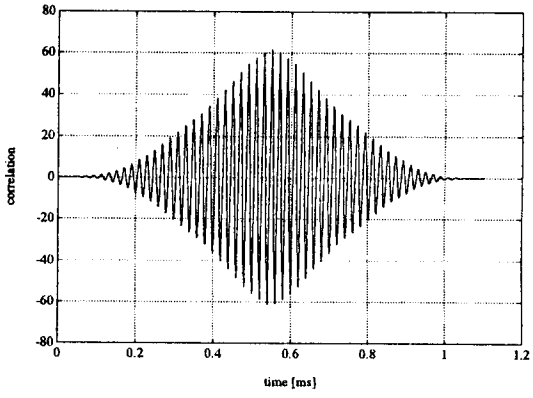

Fig. 8 Autocorrelation output of the matched filter.

As an echo pulse corresponds to a correlation peak, the echo pulse identification and arrival time measurement can be performed based on the peaks of the correlation output of the matched filter. Fig. 9 shows a typical echo signal containg several echo pulses and the correlation output of the matched filter.

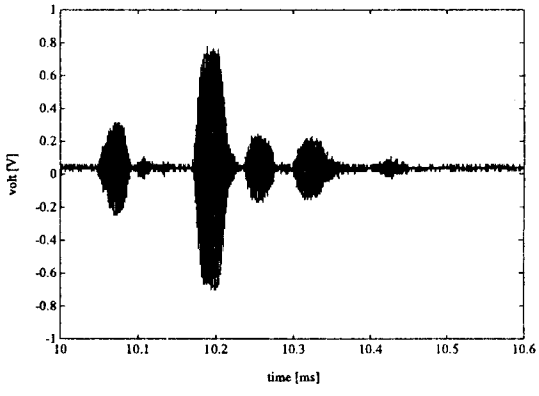

Fig. 9 (a) Typical echo of multiple pulses.

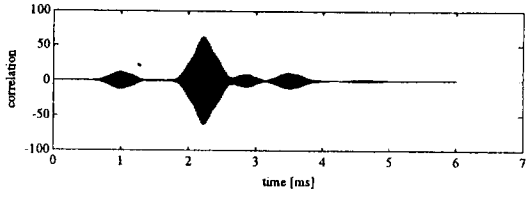

Fig. 9 (b) Correlation output of the matched filter.

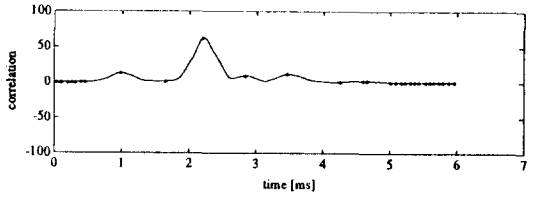

Fig. 9 (c) Correlation peaks.

We call the time of a correlation peak a *correlation peak time.* As the correlation peak occurs later than the actual echo arrival, the echo pulse arrival time is calculated by

$$t_{peak} = t_{offset} + \frac{2r}{c},$$

where t_{peak} is the cross-correlation peak time, t_{offset} is the time between the beginning of an echo pulse and the correlation peak, r is the distance to a reflector, and c is the wave propagation speed in air. Fig. 10 shows t_{offset} of a matched filter output from a rectagular pulse arrival time.

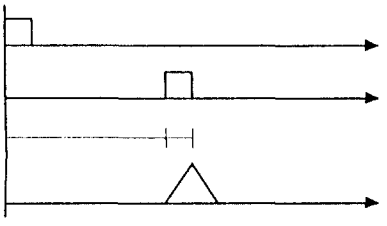

Fig. 10 Time offset between correlation peak time and echo pulse arrival time.

5. Experimental Results

5.1 Experiment Setup

We rotate the Polaroid transducer to scan horizontal plane by a stepping motor which is controlled by a computer. The echo signal is amplified by a time-variable gain amplifier, then sampled and digitized by a 8-bit digitizing oscilloscope at 400 KHz. The digital echo wave data is sent to the computer through the IEEE-488 bus for signal processing. Fig. 11 shows the experiment setup.

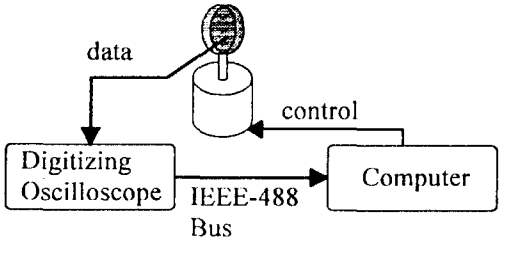

Fig. 11 Experiment setup.

5.2 Single Reflectors

First we show how the proposed method is applied to a reflector with single reflection point.

5.2.1 Transmission and Reception Pattern

The transmission beam pattern and the reception sensitivity explained in Section 3 can be measured by a pair of identical transducers. In Fig. 12, the left transducer rotates and transmits ultrasonic pulses while the right transducer receives the echo pulse and measures the magnitudes at different directions of the left transducer.

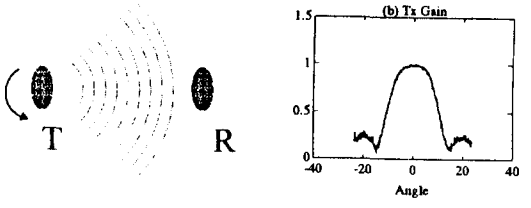

Fig. 12 Transmission pattern.

In Fig. 13, the role is reversed and the left transduer rotates and measures the magnitude of the echo pulse coming from the right transducer.

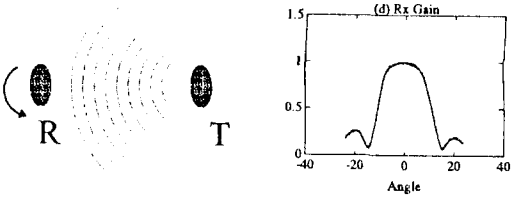

Fig. 13 Reception pattern.

5.2.2 Position Estimation

Positions of the three types reflection points are estimated by a transducer acting as a transmitter and a receiver. In Fig. 14, 15, and 16, first figures show the reflector and transducer locations. The reflection points are located at (0, 300) [cm] for all reflectors, and the transducers are located at (0,0) [cm]. The second figures show the reflector distances corresponding to the correlation peak times at different transducer directions. The direction is measured from the negative x-axis clockwise. Here, we can see that the distances corresponding to a reflector are almost invariable irrespective of the transducer directions. The third figures are the correlation magnitudes found at each transducer directions. A quadratic polynomial fitting curves are also shown. The fourth figures show the estimated positions of the reflections points. The estimated positions are seemed to be fairly accurate.

5.3 Multiple Reflectors

Generally, an object is made of more than one type of reflector. We estimated the positions of several reflection points at the same time. As before, Fig. 17 shows the

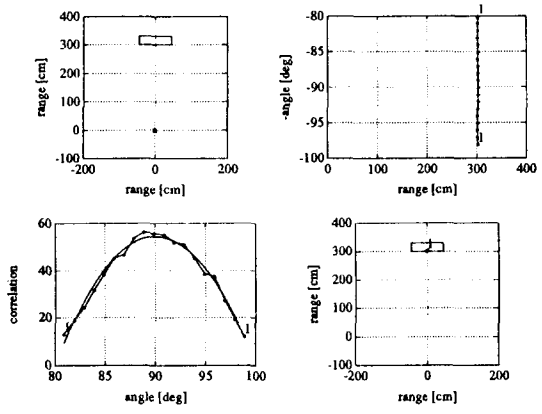

Fig. 14 Wall.

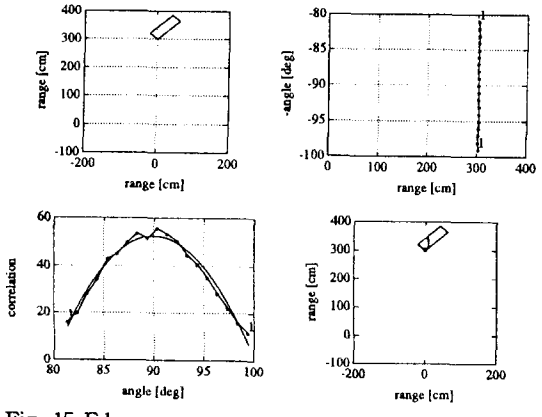

Fig. 15 Edge.

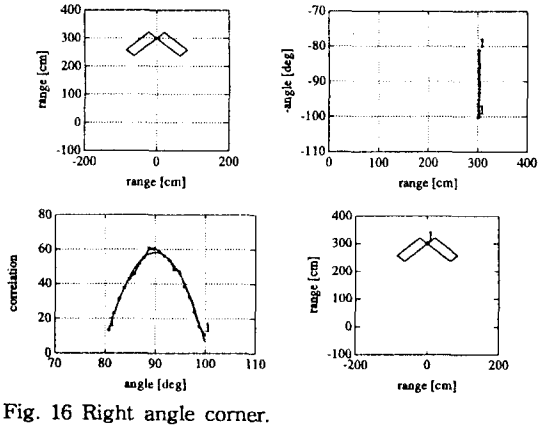

Fig. 16 Right angle corner.

configuration of the test object and the transduer, the distances corresponding to the correlation peaks found at each transducer orientation, the correlaton curves, and the estimated positions of the reflection points with respect to the test object.

5.4 Differentiation between Edge and Corner

To prove our differentiation method's validity, we tested a corner type reflector shown in Fig. 18. A transducer acting both as a transmitter and a receiver is located at

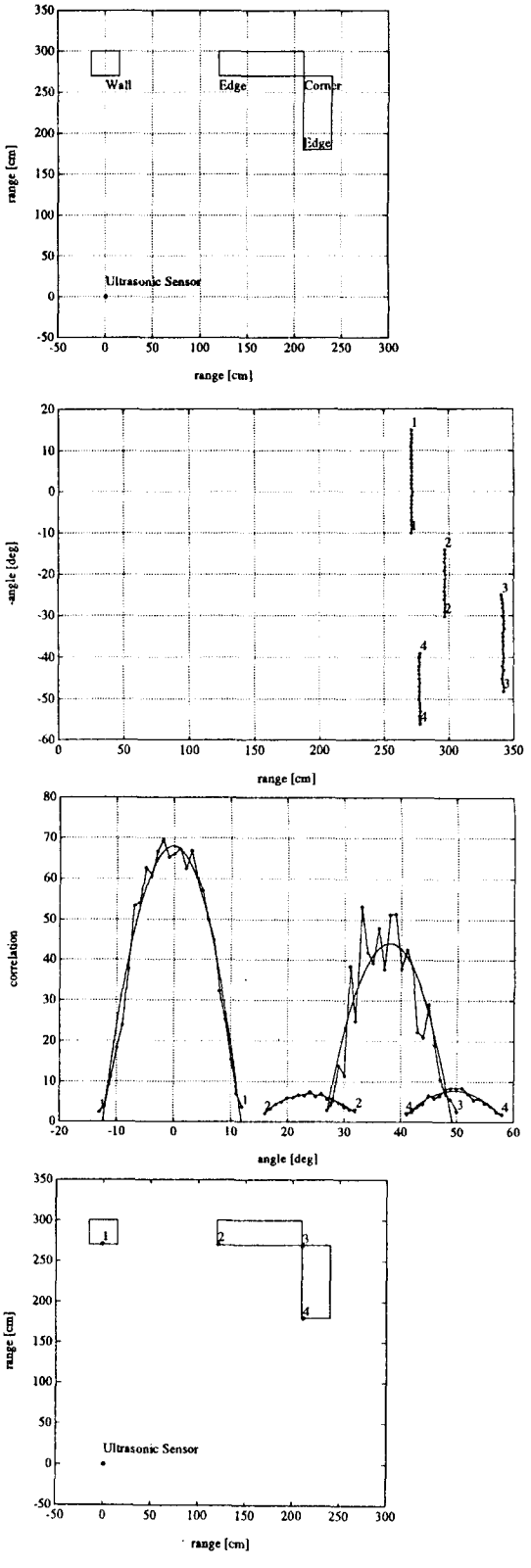

Fig. 17 Wall-edge-corner-edge object.

(0, 0), and a separate receiver R is located at (41.5, 0) [cm], and a corner vertex is located at (120, 0) [cm]. We can see that the maximum echo amplitude is acquired at the direction corresponding to a corner.

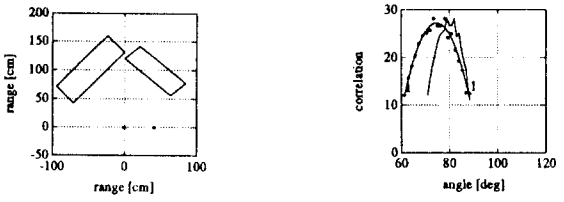

Fig. 18 Test reflector to be identified.

6. Discussion

6.1 Axial Resolution and Accuracy

The accuracy of the estimated distance to a reflection point is dependent on the correlation peak time, the offset time, and the acoustic speed in air. As the offset time and the estimated acoustic speed are all related with the correlation peak time, we discuss here only the certainty of the correlation peak time.

The correlation peak time is a function of both the shape and the arrival time of an echo pulse. But the numerous causes that change these two factors are very hard to analyze or predict. For example, the variation of transmitter circuit parameters, humidity and temperature in air, the sampling time with respect to an echo pulse are unpredictable, but they all affect the correlation peak time. Therefore, we assume a Gaussian distribution for the correlation peak time and experimentally obtain the statistical parameters. In our experiment of 1,000 repeated measurings of the correlation peak times of an object, the standard deviation was found to be 0.09 %.

Because we detect an echo pulse by finding a correlation peak, two echo pulses are identifiable as long as they provide different correlation peaks. From the linearity of correlation function, the correlation with a signal containing two echo pulses is equivalent to the sum of correlations with each pulse. Therefore, the peaks of the correlations with the pulses will be preserved if the sum of correlations does not exceed the original correlation peak values. We explain this by using exemplary pulses shown in Fig. 19. For close echo pulse as shown in the first figure, the sum of correlations is greater than the original peak values, thereby a new peak is generated. In the second figure, as two echo pulses are widely separated, the sum of cross-correlations is always smaller than the original peak values. Therefore, the original peaks are preserved. The axial resolution is defined by the range difference of two objects which maintain the correlation peaks of their echo pulses.

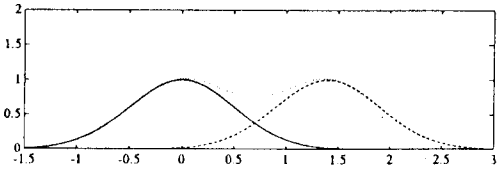

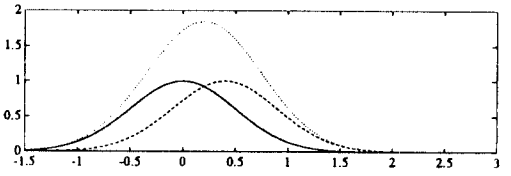

Fig. 19 Axial resolution.

6.2 Angular Resolution and Accuracy

Similar to the axial resolution, we can detect the peak of the correlation peak as long as the original peaks are preserved.

The direction to a reflector is estimated to be the angle of peak correlation magnitude, and the peak is found from a second order polynomial curve that fits to the measured correlation magnitudes with the minimum squared error. Therefore the accuracy of the estimated direction depends on the correctness of the individual correlation magnitude at each angle as well as the even symmetry of the correlation magnitude curve. If we assume the correlation magnitude is contaminated with a noise of mean zero, the curve fitting with the minimum squared error gives the best approximation to the correlation magnitude curve. Therefore, we can estimate optimally the peak of the correlation curve from the peak of the fitting curve.

If the reflecting surface is not completely specular and symmetric, the correlation curve is not symmetric, thereby some error in the estimated direction result. But this kind of error is out of scope of our current method, but we assume this error has mean of zero.

7. Conclusion

We have proposed a novel method to recognize the floor plan modeled as a collection of polygonal objects which extend toward the vertical direction. The proposed method is based on the transmission beam pattern and the reception sensitivity pattern of the ultrasonic transducer. We also suggested several schemes to implement the proposed method on the mobile robot to suit the requirement of each application such as fast processing or simple sensor configuration. The pricipal purpose of the proposed recognition method is the mobile robot's efficient indoor navigation.

The validity of the proposed method is shown through experimental results of estimated reflection points of test objects. The resolution and the accuracy of the estimated positions of the reflection points are also discussed. From the authors' point of view, the specular effect and the wide beamwidth that have been considered to be the major drawbacks of the ultrasonic sensor have positive sides as the former allow fast recognition and the later provide inherent feature selection capability.

References

[1] James L. Crowley, "Navigation for an Intelligent Mobile Robot," *IEEE Jour. of Robotics and Automation*, Vol.

RA-1, No. 1, pp. 31-41, March 1985.
[2] A. Zelinski, "Mobile Robot Map Making Using Sonar," *Jour. of Robotic Systems*, Vol. 8, No. 5, pp. 557-577, 1991.
[3] Martin Beckerman, E. M. Oblow, "Treatment of Systemetic Errors in the Processing of Wide-Angle Sonar Sensor Data for Robotic Navigation," *IEEE Trans. on Robotics and Automation*, Vol. 6, No. 2, pp. 137-145, April 1990.
[4] A. M. Flynn, "Combining Sonar and Infrared Sensors for Mobile Robot Navigation," *Int. Jour. of Robotics Research*, Vol. 7, No. 6, pp. 5-14, December 1988.
[5] Alberto Elfes, "Sonar-Based Real-World Mapping and Navigation," *IEEE Jour. of Robotics and Automation*, Vol. RA-3, No. 3, pp. 249-265, June 1987.
[6] D. W. Cho, "Certainty Grid Representation for Robot Navigation by a Bayesian Method," *ROBOTICA*, Vol. 8, pp. 159-165, 1990.
[7] Omur Bozma, Roman Kuc,"Building a Sonar Map in a Specular Environment Using a Single Mobile Sensor," *IEEE Trans. on Pattern Analysis and Machine Intelligence*, pp.1260-1269, December 1991.
[8] Herbert Peremans, Koenraad Audenaert, Jan M. Van Campenhout, "A High-Resolution Sensor Based on Tri-aural Perception," *IEEE Trans. on Robotics and Automation*, Vol. 9, No. 1, February 1993.
[9] Polaroid Corp., *Ultrasonic ranging system.* (manual and handbook), 1984[10] Lawrence E. Kinsler, Austin R. Frey, Alan B. Coppens, James V. Sanders, *Fundamentals of Acoustics 3rd Ed*, New York, U.S.A.: John Wiley & Sons, 1982, pp. 178-187.
[11] Billur Barshan, Roman Kuc,"Differentiating Sonar Reflections from Corners and Planes by Employing an Intelligent Sensor," *IEEE Trans. on Pattern Analysis and Machine Intelligence*, pp.560-569, June 1990.
[12] R. Kuc,"A Spatial Sampling Criterion for Sonar Obstacle Detection," *IEEE Trans. on Pattern Analysis and Machine Intelligence*, pp.686-690, July 1990.
[13] Roman Kuc, M. W. Siegel,"Physically Based Simulation Model for Acoustic Sensor Robot Navigation," *IEEE Trans. on Pattern Analysis and Machine Intelligence*, pp.766-778, November 1987.